

Equivalence Checking of Dynamic Quantum Circuits

Xin Hong¹, Yuan Feng^{1*}, Sanjiang Li^{1*} and Mingsheng Ying^{1,2,3*}

¹*Centre for Quantum Software and Information, University of Technology Sydney, Australia*

²*State Key Laboratory of Computer Science, Institute of Software, Chinese Academy of Sciences, China*

³*Department of Computer Science and Technology, Tsinghua University, China*

Abstract—Despite the rapid development of quantum computing these years, state-of-the-art quantum devices still contain only a very limited number of qubits. One possible way to execute more realistic algorithms in near-term quantum devices is to employ dynamic quantum circuits, in which measurements can happen during the circuit and their outcomes are used to control other parts of the circuit. This technique can help to significantly reduce the resources required to achieve a given accuracy of a quantum algorithm. However, since this type of quantum circuits are more flexible, their verification is much more challenging. In this paper, we give a formal definition of dynamic quantum circuits and then propose to characterise their functionality in terms of ensembles of linear operators. Based on this novel semantics, two dynamic quantum circuits are equivalent if they have the same functionality. We further propose and implement two decision diagram-based algorithms for checking the equivalence of dynamic quantum circuits. Experiments show that embedding classical logic into conventional quantum circuits does not incur significant time and space burden.

Index Terms—Quantum circuits, quantum measurements, dynamic quantum circuits, equivalence checking

I. INTRODUCTION

The past five years have witnessed significant breakthroughs in building small-scale quantum devices and the largest quantum computers now have above 50 qubits. It is widely believed that near-term quantum devices will remain very limited in terms of the number of qubits they may have. Furthermore, these quantum devices also suffer from noises and short coherence time. This makes it highly difficult to implement large practical quantum circuits.

To fully exploit the power of quantum computing in these noisy intermediate-scale quantum (NISQ) [1] devices, several prominent approaches have been proposed to overcome the tight scale restriction. These include the quantum network approach [2], which connects multiple small-scale quantum computers, hybrid quantum/classical algorithms (see [3] for a survey), which join quantum computers with classical computers, and dynamical quantum circuits [4], [5], which try to build classical logic directly into quantum circuits.

Conventionally, a quantum circuit starts with a set of qubit initialisation, then an ordered sequence of qubit gates, and ends with or without measurements. As pointed out in [5], in these conventional quantum circuits, classical logic is not performed within the coherence time of the qubits.

Dynamic quantum circuits are circuits in which measurements can be performed in the middle of the circuit and the measurement results are then used to control some quantum gates to be applied afterwards; early examples include quantum teleportation [6], [7], [8], [9] and quantum error correction (QEC) [10], [11], [12], [13]. For QEC, the syndrome of an encoded quantum state is detected through a set of measurements, and a series of quantum gates are then applied to the error quantum state according to the measurement results, and thus the quantum state is recovered.

The dynamic quantum circuit technique has also been used in extending the lifetime of quantum bits [14], resetting qubits [15], realising non-elementary quantum gates [4], [16], generating entanglement [17], [18], and embedding the classical real-time logic into quantum systems [5], [19]. Experiments in [5] show that dynamic circuits can indeed offer a ‘substantial and tangible advantage’ on current noisy quantum hardware.

As dynamic quantum circuits will play a more important and central role in the near-future quantum computing, their verification becomes an imperative problem. Still lacking a formal definition of dynamic quantum circuits, it is not surprise that this problem is completely untouched. This paper provides a first such attempt and focuses on the equivalence checking of dynamic quantum circuits. Similar to the case of classical circuits, equivalence checking is essential to maintain the correctness of a quantum circuit. Moreover, as quantum circuits become larger and larger, they are more and more error-prone. It is necessary to provide automatic tools for checking the equivalence of different quantum circuit designs. For conventional quantum circuits, the decision diagram-based approach plays a prominent role, see, e.g., [20], [21], [22], [23]. For two quantum circuits, their equivalence is simply reduced to checking if the corresponding decision diagram representations are identical. However, due to the existence of classical control, it is not clear if all these decision diagram approaches can be directly applied to checking the equivalence of two dynamic quantum circuits.

In this paper, we first give a formal definition of dynamic quantum circuits and lay a rigorous foundation for our discussion by characterising their functionalities in terms of ensembles of linear operators. Then we formally define the notion of equivalence of dynamic quantum circuits and present two special cases, called m- and q-equivalences, which cover most, if not all, existing realistic dynamic quantum circuits.

*Email: {yuan.feng,sanjiang.li,mingsheng.ying}@uts.edu.au.

The m-equivalence focuses on the measurement results while the q-equivalence cares only about the output quantum states. The quantum phase estimation (QPE) algorithm and QEC are, respectively, representative examples of the application scenarios of the two equivalence definitions. Then, we propose and implement two algorithms for checking the m- and q-equivalences, based on the tensor decision diagram (TDD) [23]. As a data structure, TDD provides a compact and canonical representation for tensors and, in particular, quantum circuits. It can be used in many design automation tasks, e.g., simulation [23] and equivalence checking [24], for quantum circuits. In order to represent dynamic quantum circuits, what we need to do is to (a) represent measurements and classically controlled gates as tensors and construct their TDDs and (b) represent Boolean functions as TDDs. This is natural as TDDs are generalisations of binary decision diagrams [25] and tensors are, in a sense, generalisations of Boolean functions.

Our main contributions are summarised as follows:

- 1) A formal definition of dynamic quantum circuits and the characterisation of their functionalities in terms of ensembles of linear operators;
- 2) A formal definition of dynamic quantum circuit equivalence and two special cases, viz., m- and q-equivalences, covering most real-world application scenarios;
- 3) Implementation of two TDD-based algorithms for checking the m- and q-equivalences.

In the remainder of this paper, we first recall some basic concepts of quantum computing and tensor networks in Sec. II, and then present our formal definitions of dynamic quantum circuits and their equivalence in Sec. III. Algorithms for checking the m- and q-equivalences of dynamic quantum circuits are described in Sec. IV, followed by experiments and numerical results in Sec. V and conclusion in Sec. VI.

II. BACKGROUNDS

In this section, we recall some basic concepts from quantum computing and tensor networks. For quantum computing, we adopt notations from [26], [27]. Interested readers may consult [28], [29] for more details in tensor networks.

A. Quantum Circuits

A (conventional) quantum circuit is a series of quantum gates, which are modelled by unitary matrices, acting on qubit (quantum bit) variables. For each qubit q , we write \mathcal{H}_q for its state Hilbert space, which is two-dimensional. Using the Dirac notation, a pure state of q is represented by $|\psi\rangle = \alpha_0|0\rangle + \alpha_1|1\rangle$ with complex numbers α_0 and α_1 satisfying $|\alpha_0|^2 + |\alpha_1|^2 = 1$. A sequence $\bar{q} = q_1, \dots, q_n$ of distinct qubit variables is called a quantum register. Its state Hilbert space is the tensor product $\mathcal{H}_{\bar{q}} = \bigotimes_{i=1}^n \mathcal{H}_{q_i}$, which is 2^n -dimensional. Thus, an n -qubit state can be also represented by an 2^n -dimensional vector $|\psi\rangle = (\alpha_0, \dots, \alpha_{2^n-1})^T$. A unitary transformation on \bar{q} is modelled by a $2^n \times 2^n$ unitary matrix U . This transformation is also called an n -qubit quantum gate and denoted as $G \equiv U[\bar{q}]$. We use the notation $qv(G)$ to represent the qubits that the gate is operated on. A quantum circuit can be formed

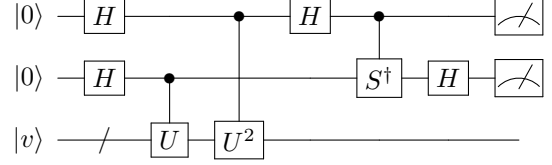


Fig. 1. Quantum circuit for 2-qubit Phase Estimation. The wires from top to bottom represent qubits q_1 , q_2 , and r respectively.

by a sequence of quantum gates: $C \equiv G_1; \dots; G_d$, and the quantum register of C is denoted $qv(C) = \bigcup_{i=1}^d qv(G_i)$.

To read out the information obtained by running a quantum circuit, measurement are sometimes applied at the end of a circuit. Let $\bar{q} = q_1, \dots, q_n$ be a quantum register. A measurement on $\mathcal{H}_{\bar{q}}$ is a collection $\{M_m\} \subseteq \mathcal{L}(\mathcal{H}_{\bar{q}})$ of operators satisfying the normalisation condition: $\sum_m M_m^\dagger M_m = I_{\mathcal{H}_{\bar{q}}}$, where $I_{\mathcal{H}_{\bar{q}}}$ is the identity matrix in $\mathcal{H}_{\bar{q}}$ and M_m (the index m stands for the measurement outcome) are called measurement operators. If the state of a quantum system is $|\psi\rangle$ immediately before the measurement, then, for each outcome m , the probability that m occurs is $p(m) = \langle\psi| M_m^\dagger M_m |\psi\rangle$ and the state of the system after observing m is $|\psi_m\rangle = M_m |\psi\rangle / \sqrt{p(m)}$.

The basic measurement used in this paper is the measurement in the computational basis, which is formed by two operators $M_0 = |0\rangle\langle 0|$, $M_1 = |1\rangle\langle 1|$ for a single qubit. If the qubit before the measurement was in state $|\psi\rangle = \alpha_0|0\rangle + \alpha_1|1\rangle$, then the probability of obtaining outcome $m \in \{0, 1\}$ is $p(m) = \langle\psi| M_m^\dagger M_m |\psi\rangle = |\alpha_m|^2$, and the state after measurement is $M_m |\psi\rangle / \sqrt{p(m)} = |m\rangle$.

Example 1. Depicted in Fig. 1 is a quantum circuit which implements the 2-qubit Phase Estimation [26], where

$$H = \frac{1}{\sqrt{2}} \begin{bmatrix} 1 & 1 \\ 1 & -1 \end{bmatrix}, \quad S^\dagger = \begin{bmatrix} 1 & 0 \\ 0 & -i \end{bmatrix},$$

U is a unitary matrix, and $|v\rangle$ is an eigenstate of U ; that is, $U|v\rangle = e^{2\pi i \phi} |v\rangle$ for some $\phi \in [0, 1)$. Here the two measurements at the end are both in the computational basis, and the observed outcomes give the best two-bit approximation of ϕ with high probability. In particular, if $\phi = 0.\phi_1\phi_2$ is the binary representation of ϕ , then we will obtain ϕ_1 in q_1 and ϕ_2 in q_2 with probability 1.

B. Tensor Networks

A *tensor* is a multidimensional linear map associated with a set of indices. In this paper, we assume that each index takes value in $\{0, 1\}$ and tensors take values from \mathbb{C} , the field of complex numbers. That is, a tensor ϕ with index set $I = \{x_1, \dots, x_n\}$ is a mapping from $\{0, 1\}^I$ to \mathbb{C} . It is also denoted by $\phi_{x_1 \dots x_n}$ or $\phi_{\vec{x}}$. The value of ϕ under an assignment $\{x_i \mapsto a_i, 1 \leq i \leq n\}$ is denoted by $\phi_{x_1 \dots x_n}(a_1, \dots, a_n)$, or $\phi_{\vec{x}}(\vec{a})$, or even $\phi(\vec{a})$ for simplification. The number n of the indices of a tensor is called its *rank*. Scalars, 2-dimensional vectors, and 2×2 matrices are tensors with rank 0, 1, and 2, respectively.

The most important tensor operation is *contraction*. For any two tensors, their contraction is a tensor obtained by summing up over shared indices. For example, let γ_{x_1, x_2} and

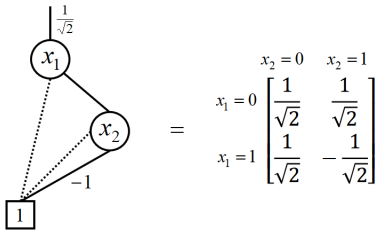


Fig. 2. TDD of the H gate.

ξ_{x_2, x_3} be two tensors which share a common index x_2 . Then their contraction is a new tensor ϕ_{x_1, x_3} with $\phi_{x_1, x_3}(a_1, a_3) = \sum_{a_2 \in \{0,1\}} \gamma_{x_1, x_2}(a_1, a_2) \cdot \xi_{x_2, x_3}(a_2, a_3)$. When both γ and ξ are 2×2 matrices, contraction is exactly matrix multiplication.

Another useful tensor operation is *slicing*, which corresponds to the cofactor operation of Boolean functions. Let ϕ be a rank $n+1$ tensor. Then its slicing w.r.t. $x = c$ for index x and $c \in \{0,1\}$ is a rank n tensor. For example, let ϕ be a tensor with index set $I = \{x, x_1, \dots, x_n\}$. The slicing of ϕ w.r.t. $x = c$ is a tensor $\phi|_{x=c}$ over $I' = \{x_1, \dots, x_n\}$ given by $\phi|_{x=c}(\vec{a}) := \phi(c, \vec{a})$, for any $\vec{a} \in \{0,1\}^n$. We call $\phi|_{x=0}$ and $\phi|_{x=1}$ the *negative* and *positive* slicing of ϕ with respect to x , respectively.

Quantum states and quantum gates can both be represented by tensors. For example, the quantum state $|0\rangle$ can be represented by a rank 1 tensor ϕ_x with $\phi_x(0) = 1, \phi_x(1) = 0$, and the H gate in Example 1 is represented by the rank 2 tensor with $\phi_{x_1, x_2}(00) = \phi_{x_1, x_2}(01) = \phi_{x_1, x_2}(10) = 1/\sqrt{2}, \phi_{x_1, x_2}(11) = -1/\sqrt{2}$. Clearly, each quantum circuit can be represented by the tensor obtained by contracting all its gates and input/output states.

A set of tensors can be connected to form a network. A *tensor network* is an undirected graph $G = (V, E)$ with zero or multiple open edges, where each vertex v in V represents a tensor and each edge a common index associated with the two adjacent tensors. Tensors sharing the same index should be contracted, and this contraction leads to a rank m tensor if there are m open edges in the tensor network. In this way, quantum circuits are special tensor networks with every node representing a quantum gate or a quantum state.

C. Tensor Decision Diagrams

The most commonly used equivalence checking methods for conventional quantum circuits are based on decision diagram [20], [21], [22], [23]. The current paper adopts the tensor decision diagrams (TDDs) proposed in [23] which can represent tensors and, thus, quantum circuits, in a canonical and compact way. Given a tensor ϕ , the root node r_ϕ of its TDD Φ is labelled with an index of ϕ and the two successors of r_ϕ represent the negative (0-successor) and positive (1-successor) slicing of ϕ w.r.t. this index. The value of ϕ under an assignment is obtained by multiplying the weights of the corresponding path in Φ .

Example 2. Fig. 2 shows the TDD of the H gate. In this diagram, dotted lines correspond to the 0-successors, and solid lines the 1-successors. The weight $1/\sqrt{2}$ on the incoming edge of the root is called the weight of the TDD. The dotted line of the root node (labelled with index x_1) leads to the terminal node 1, meaning that when the index x_1 takes value 0, the tensor will take value $1/\sqrt{2} \times 1 = 1/\sqrt{2}$. All 1-weights are omitted in the diagram.

A TDD tdd is determined by its weight $tdd.weight$ and the root node $tdd.root$, every node in a TDD has an index $node.index$ and, except the terminal node, two successors $node.succ_0$ and $node.succ_1$. Two TDDs tdd_1 and tdd_2 are *identical* iff $tdd_1.weight = tdd_2.weight$ and $tdd_1.root = tdd_2.root$. As TDD provides canonical representation for conventional quantum circuits [23], to check if two such circuits are equivalent, we first calculate their TDDs and then compare their weights and nodes. If their TDDs are identical, then these two quantum circuits are equivalent.

III. DYNAMIC QUANTUM CIRCUITS

Informally speaking, a dynamic quantum circuit is a conventional circuit with measurements in the middle and the subsequent circuits can depend on the measurement outcomes [5]. To establish a rigorous foundation for verification of such circuits, we next give a formal definition, generalising the notion of quantum circuits with measurements in [27] by introducing more flexible control flows.

A. Dynamic Quantum Circuits

Definition 1 (Dynamic Quantum Circuits). A *dynamic quantum circuit* (dQC) is defined inductively as follows:

- 1) Each conventional quantum circuit C acting on qubits \bar{q} is a dQC , and $qv(C) = \bar{q}$;
- 2) Let M be the measurement in computational basis of $\mathcal{H}_{\bar{r}}$ and, for each $0 \leq i < 2^t$, C_i a dQC with $\bar{r} \cap qv(C_i) = \emptyset$. Let $f : \{0,1\}^{|\bar{r}|} \rightarrow \{0,1\}^t$ be a Boolean function. Then

$$C \equiv \text{if } (\square i \cdot f(M[\bar{r}]) = i \rightarrow C_i) \text{ fi}$$

is a dQC , and $qv(C) = \bigcup_i qv(C_i)$.

- 3) If C_1 and C_2 are $dQCs$, then so is $C_1; C_2$ and $qv(C_1; C_2) = qv(C_1) \cup qv(C_2)$.

Intuitively, the construct in Clause 2 of the above definition denotes a dQC which first measures the qubits in \bar{r} according to the measurement M . If f maps the measurement outcome to m , then C_m is chosen to be executed subsequently. Furthermore, Clause 3 describes sequential composition of $dQCs$.

Similar to conventional quantum circuits, a dynamic circuit is sometimes accompanied with a fixed input state for some of its qubits. Furthermore, a specific set of qubits will be discarded at the end and their quantum states are not included in the circuit output. To incorporate this situation, in the following we denote a dQC as a tuple

$$(C[\bar{q}], |\psi\rangle, \bar{i}, \bar{o})$$

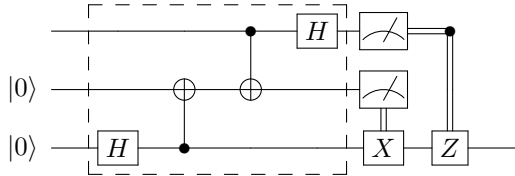


Fig. 3. Quantum circuit for Teleportation. The wires from top to bottom represent qubits q , q_1 , and q_2 respectively.

where $\bar{q} = qv(C)$, and \bar{i} and \bar{o} are both subsets of \bar{q} indicating the (principal) input qubits and output qubits, respectively, and $|\psi\rangle \in \mathcal{H}_{\bar{q} \setminus \bar{i}}$ is its fixed input state.

Definition 2 (Functionality of dQCs). *The functionality of a dQC C , denoted $\llbracket C \rrbracket$, is an ensemble of linear operators on $\mathcal{H}_{qv(C)}$ defined inductively as follows:*

- 1) *If C is a conventional quantum circuit, then $\llbracket C \rrbracket = \{U\}$ where U is the unitary operator computed by C in the usual way;*
- 2) *Let*

$$C \equiv \text{if } (\square i \cdot f(M[\bar{r}]) = i \rightarrow C_i) \text{ fi}$$

and $\llbracket C_i \rrbracket = \{F_{i,k} : k \in J_i\}$ for each i . Then $\llbracket C \rrbracket$ is an ensemble

$$\left\{ |j\rangle_{\bar{r}} \langle j| \otimes F_{f(j),k} : 0 \leq j < 2^{|\bar{r}|}, k \in J_{f(j)} \right\}.$$

- 3) *If C_1 and C_2 are dQCs with $\llbracket C_1 \rrbracket = \{E_i : i \in I\}$ and $\llbracket C_2 \rrbracket = \{F_j : j \in J\}$, then*

$$\llbracket C_1; C_2 \rrbracket = \{F_j E_i : i \in I, j \in J\}.$$

Finally, for dQCs where certain input qubits are with fixed initial states and certain output qubits are discarded, the functionality is defined as follows. Let $\llbracket C \rrbracket = \{F_j : j \in J\}$. Then $\llbracket (C[\bar{q}], |\psi\rangle, \bar{i}, \bar{o}) \rrbracket$ is a super-operator from $\mathcal{H}_{\bar{i}}$ to $\mathcal{H}_{\bar{o}}$ such that for any $\rho \in \mathcal{D}(\mathcal{H}_{\bar{i}})$,

$$\llbracket (C[\bar{q}], |\psi\rangle, \bar{i}, \bar{o}) \rrbracket(\rho) = \text{tr}_{\bar{q} \setminus \bar{o}} \left[\sum_{j \in J} F_j (|\psi\rangle \langle \psi| \otimes \rho) F_j^\dagger \right].$$

Here $\text{tr}_{\bar{q} \setminus \bar{o}}$ is the partial trace operation which discards the $\bar{q} \setminus \bar{o}$ register and takes the reduced quantum state in the remaining part (the \bar{o} register).

Example 3. Fig. 3 gives an example of dynamic quantum circuit. This circuit is the well known circuit for quantum teleportation which transfers a qubit by just sending two classical bits of information. Let the (conventional) circuit in the dashed box be $C_0[q, q_1, q_2]$, and $D_0 \equiv I$, $D_1 \equiv X[q_2]$, $D_2 \equiv Z[q_2]$, and $D_3 \equiv ZX[q_2]$. Then the whole dynamic circuit can be written as $(C[q, q_1, q_2], |00\rangle_{q_1, q_2}, q, q_2)$ where

$$C \equiv C_0; \text{if } (\square i \cdot M[q, q_1] = i \rightarrow D_i) \text{ fi}$$

and $M = \sum_{i=0}^3 |i\rangle \langle i|$ is the 2-qubit measurement in the computational basis. It is easy to check that for any $\rho \in \mathcal{D}(\mathcal{H}_q)$, $\llbracket (C[q, q_1, q_2], |00\rangle_{q_1, q_2}, q, q_2) \rrbracket(\rho) = \rho$.

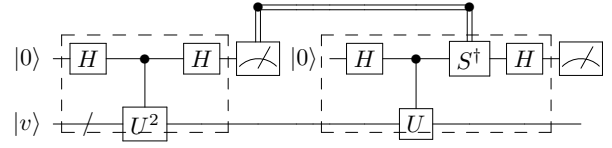


Fig. 4. Dynamic quantum circuit for 2-qubit phase estimation. The wires with input $|0\rangle$ from left to right represent qubits q_1 and q_2 , respectively, and the wire on the bottom denotes qubit r .

The circuit in Fig. 1 can also be transformed to a dynamic quantum circuit, since the controlled- S gate in the circuit do not change the measurement result of the first qubit. Thus, we can conduct the measurement before the controlled- S^\dagger gate and replace it with a classically controlled gate.

Example 4. Fig. 4 shows the dynamic quantum circuit version of the phase estimation shown in Fig. 1. Let the (conventional) circuit in the left dashed box be $C_0[q_1, r]$, the circuit in the right dashed box be $D_1[q_2, r]$, and the circuit in the right dashed box without the S^\dagger gate be $D_0[q_2, r]$. Then the whole dynamic circuit can be written as $(C[q_1, q_2, r], |00\rangle_{q_1, q_2} |v\rangle_r, \emptyset, q_1 q_2)$ where

$$C \equiv C_0; \text{if } (\square i \cdot M[q_1] = i \rightarrow D_i) \text{ fi}$$

and M is the 1-qubit computational basis measurement. Note that there is no principal input for this circuit. It is easy to check that $\llbracket (C[q_1, q_2, r], |00\rangle_{q_1, q_2} |v\rangle_r, \emptyset, q_1 q_2) \rrbracket = |\phi_1 \phi_2\rangle \langle \phi_1 \phi_2|$ provided that $U|v\rangle = e^{2\pi i 0 \cdot \phi_1 \phi_2} |v\rangle$.

B. Equivalence of dQCs

With Definition 2, we can now define the equivalence of two dQCs as follows.

Definition 3 (Equivalence of dQCs). *Two dynamic quantum circuits $(C[\bar{q}], |\psi\rangle, \bar{i}, \bar{o})$ and $(C'[\bar{q}'], |\psi'\rangle, \bar{i}, \bar{o})$ with the same principal input and output qubits are equivalent if their functionality are the same; that is,*

$$\llbracket (C[\bar{q}], |\psi\rangle, \bar{i}, \bar{o}) \rrbracket = \llbracket (C'[\bar{q}'], |\psi'\rangle, \bar{i}, \bar{o}) \rrbracket.$$

In this paper we are particularly concerned with the equivalence of two special classes of dynamic quantum circuits, which cover most real-world applications. In the first class, all input states are fixed (i.e. $\bar{i} = \emptyset$) and all principal output qubits have been measured during execution of the circuit (the outcomes were or were not used in subsequent circuits). Typical examples include phase estimation in Example 4 and the period finding algorithm. Therefore, the output can be regarded as purely classical information; more precisely, it is merely a probability distribution over $\{0, 1, \dots, 2^{|\bar{o}|} - 1\}$. We call the equivalence of such dynamic circuits **m-equivalence**. It is not difficult to see that circuits depicted in Figs. 1 and 4 are m-equivalent.

In the second class of dynamic circuits, measurement outcomes during the execution process were used to control subsequent circuits, and do not constitute a part of the output of the entire circuit. Furthermore, the output quantum state is independent of the measurement outcomes. Typical examples

in this class include teleportation in Example 3 and error correction. We call the equivalence of such dynamic circuits **q-equivalence**. Again, it is easy to show that the circuit depicted in Fig. 3 is q-equivalent to the dynamic circuit $(SWAP[q, q_2], |0\rangle_{q_2}, q, q_2)$ which transfers the state of q to q_2 by employing the swap gate.

IV. TDD-BASED EQUIVALENCE CHECKING

In this section, we present our methods and algorithms for checking the m- and q-equivalence of dynamic quantum circuits. The idea is to represent each dynamic quantum circuit as a TDD and then compare if they are identical. To this end, we first consider how to represent measurements and classically controlled gates as tensors, and then consider how to represent Boolean functions as TDD. In this way, we shall have ensured that every element in a dynamic quantum circuit can be represented as a TDD. As a consequence, the TDD representation of the whole dynamic quantum circuit can be obtained by TDD contractions.

A. Tensor Representation of Measurements and Classically Controlled Gates

Note that measurement in the computational basis of a multi-qubit system can be decomposed into those of the 1-qubit subsystems. Furthermore, the probability of measuring a qubit can be read out from the TDD representation of a quantum circuit. Therefore, there is no need to really operate a measurement if it is at the end of the circuit so will not be used to control other parts of the circuit.

More precisely, we regard each measurement as a rank 2 COPY tensor $\phi_{x,y} = I$ provided that the measurement result is not used to control other parts of the circuit. Otherwise, we regard it as a rank 3 COPY tensor $\phi_{c,x,y}$, where $\phi(000) = \phi(111) = 1$ and it equals 0 in all other cases. In this representation, c captures the behaviour of the measurement result and x, y capture the behaviour of the quantum state. When the measurement result is $c = 0$, the tensor is exactly $\phi|_{c=0} = |0\rangle\langle 0| = M_0$; and if $c = 1$, then it equals to $\phi|_{c=1} = |1\rangle\langle 1| = M_1$.

A classically controlled- U gate can also be interpreted as a rank 3 tensor $\psi_{c,x',y'}$, where $\psi|_{c=0} = I$ and $\psi|_{c=1} = U$. That is, when the measurement result (i.e., the classical control bit) is 1 the quantum gate U will be applied, and, otherwise, it does nothing. Suppose M is the measurement whose outcomes are used to control U . Then the contraction of ψ with the tensor that represents M gives a rank 4 tensor $|0\rangle\langle 0|\otimes I + |1\rangle\langle 1|\otimes U$, which is equivalent to a quantum controlled- U gate.

The TDD of a dynamic quantum circuit can be obtained by contracting all tensors in the circuit.

Example 5. Consider the circuit in Fig. 4. The contraction of the first measurement with the classically controlled- S^\dagger gate equals to the quantum controlled- S^\dagger gate in Fig. 1 and the measurement in the end of the circuit is equivalent to an identity matrix. Thus, contracting all these tensors is just equivalent to contracting all tensors in Fig. 1 before measurement, which is also equivalent to contracting all

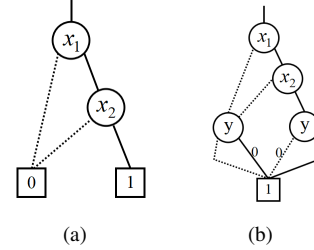


Fig. 5. The BDD (a) and TDD (b) representations of the logical AND gate.

tensors in Fig. 1 (including the measurement). This shows that these two dynamic quantum circuits are equivalent.

B. Representing Boolean Functions as TDDs

In a dynamic quantum circuit, measurement results are usually sent through a classical combinational circuit and the outputs are used to control the quantum system (see Clause 2 of Definition 1 for the formal description). Thus, we need also provide TDD representations for the classical logic.

A classical logic gate is in essence a Boolean function $f : \{0, 1\}^n \rightarrow \{0, 1\}$. To represent f as a tensor, we introduce a new index y to describe its output signal. Then, f can be described as a tensor $\phi : \{0, 1\}^{n+1} \rightarrow \{0, 1\}$ with index set $\{x_1, \dots, x_n, y\}$, where $\phi_{x_1, \dots, x_n, y} = 1$ iff $f(x_1, \dots, x_n) = y$. We call this the tensor representation of f .

For example, consider the logic AND gate whose Boolean function is $f(x_1, x_2) = x_1 \wedge x_2$, which takes value 1 iff both x_1 and x_2 take values 1. Introducing a new index y to represent the output signal of this gate, f can be represented by a tensor $\phi_{x_1 x_2 y}$, where $\phi(000) = \phi(010) = \phi(100) = \phi(111) = 1$ since $f(00) = f(01) = f(10) = 0$ and $f(11) = 1$, and the tensor takes value 0 for all other combinations.

Let $\varphi_{x_1, \dots, x_n, y_1}$ and $\gamma_{x_1, \dots, x_n, y_2}$ be the tensor representations of two Boolean functions. Suppose y_1 and y_2 are used as input signals into another logic gate with tensor representation $\xi_{y_1, y_2, z}$. The contraction of the three tensors on y_1, y_2 is

$$\phi_{x_1, \dots, x_n, z} = \sum_{y_1, y_2} \varphi_{x_1, \dots, x_n, y_1} \cdot \gamma_{x_1, \dots, x_n, y_2} \cdot \xi_{y_1, y_2, z}.$$

Since, φ, γ, ξ equal 1 iff $x_1, \dots, x_n, y_1, y_2, z$ coincide with the input and output behaviour of the Boolean function, thus, the contracted tensor $\phi_{x_1, \dots, x_n, z}$ equals 1 iff x_1, \dots, x_n, z coincide with the input-output behaviour of connecting the two outputs y_1, y_2 to the inputs of the last logic gate, i.e., ϕ is the tensor representation of the combined circuit.

According to this observation, the behaviour of a classical circuit can thus be captured using the contraction of tensor networks. In practice, the Boolean function is often given as a binary decision diagram (BDD) [25]. In this case, it can be easily transformed to a TDD by introducing two nodes which are labelled with the output index of the classical circuit and represent the tensors $\phi_y(0) = 0, \phi_y(1) = 1$ and $\phi_y(1) = 0, \phi_y(0) = 1$ respectively.

Example 6. Fig. 5 (a) is the BDD representation of the logic AND gate. For this gate, introduce an index y to describe its

output, then redirect every edge linked to terminal node 0 to a node labelled with y with 0-successor 1 and 1-successor 0, and redirect every edges linked to terminal node 1 to a node labelled with y with 0-successor 0 and 1-successor 1, such as shown in Fig. 5 (b). Then this TDD captures the behaviour of the Boolean function and can be used to do further calculation.

In this way, the TDD representation of the classical circuit can be calculated from its Boolean function or transformed from its BDD representation. Contracting the TDDs of the classical parts and quantum parts of the dynamic circuit finally gives the TDD of the whole circuit.

C. Basic Algorithms

The direct method for checking the equivalence of two dynamic quantum circuits is to first calculate their TDD representations and then compare.

m-Equivalence. For m-equivalence, we have to extract the probabilities of observing different measurement outcomes from the TDD of the dynamic quantum circuit. Suppose the two TDDs to be compared are constructed using the same index order, and all output qubits are on the top of the TDDs. For a sequence s of measurement outcomes, let r_s be the node reached from the root of the TDD following the path determined by s . The probability of s is exactly the norm of the sub-TDD rooted at r_s weighted by the magnitude of the weight accumulated along the path. Here the norm of a TDD is obtained by contracting the TDD with its conjugate transpose, which has the same structure but with all corresponding weights conjugated. Finally, the circuits represented by the two TDDs are m-equivalent if, for each sequence s of measurement outcomes, the corresponding probabilities determined by s in these two TDDs are equal. Alg. 1 gives the detailed steps of this process.

q-Equivalence. For q-equivalence, we ignore probabilities of the measurement results and require that the state remained after measurements are independent of the measurement results. We need check if the output state is the same for all input states. If so, the two circuits are q-equivalent. Again, we assume that the measured qubits are on the top of the two TDDs and the two TDDs use the same index order. Alg. 2 gives the detailed procedure of this process. In the algorithm, we recursively visit the nodes of a TDD and add them to a set if the index of this node is not a measurement index. Since nodes in the TDD that represent the same tensor share the same address, thus, if the two circuits are q-equivalent, then, finally, the set will become a singleton. The algorithm uses this observation to determine the equivalence.

D. Optimisation

The equivalence of dynamic quantum circuits can be checked in a divide-and-conquer manner. Suppose the circuits are partitioned into corresponding sub-circuits. If two equivalent corresponding sub-circuits are found, we delete them from the circuits and check the remaining parts. The circuit partition scheme has been used in tensor network-based quantum circuit simulation [30] and TDD calculation [23]. In this paper, we

Algorithm 1 $m_eq(tdd_1, tdd_2)$

Require: tdd_1, tdd_2 are the TDDs of two dynamic circuits
Ensure: return **true** iff the circuits represented by tdd_1 and tdd_2 are m-equivalent

```

if  $tdd_1 = tdd_2$  then
    return true
end if
 $x \leftarrow \min(tdd_1.root.index, tdd_2.root.index)$ 
if  $x$  is not a measurement index then
     $N_1, N_2 \leftarrow$  norm of  $tdd_1$ , norm of  $tdd_2$ 
    return  $N_1 = N_2$ 
end if
for  $i = 1, 2$  do
    if  $tdd_i.root.index = x$  then
         $w_i \leftarrow tdd_i.weight$ 
         $L_i \leftarrow |w_i| \cdot tdd_i.root.succ_0$ 
         $H_i \leftarrow |w_i| \cdot tdd_i.root.succ_1$ 
    else
         $L_i, H_i \leftarrow tdd_i$ 
    end if
end for
return  $m\_eq(L_1, L_2) \wedge m\_eq(H_1, H_2)$ 

```

Algorithm 2 $q_eq(tdd_1, tdd_2)$

Require: tdd_1, tdd_2 are the TDDs of two dynamic circuits
Ensure: return **true** iff the circuits represented by tdd_1 and tdd_2 are q-equivalent

```

nodes  $\leftarrow$  get_nodes( $tdd_1$ )  $\cup$  get_nodes( $tdd_2$ )
return  $|\text{nodes}| = 1$ 

/* get_nodes subroutine */
Subroutine get_nodes( $tdd$ )
 $r \leftarrow tdd.root$ 
if  $r.index$  is a measurement index then
    return get_nodes( $r.succ_0$ )  $\cup$  get_nodes( $r.succ_1$ )
else
    return  $\{r\}$ 
end if

```

consider a simple circuit partition scheme in which the circuit is partitioned qubit-by-qubit. More precisely, we first calculate the two tensors corresponding to the first qubit, compare them and then consider the second qubit and so on.

For m-equivalence, if the tensors corresponding to a same qubit of the two circuits are identical, they can be discarded. This is because, if such two tensors are identical, then the distributions of measuring this qubit are identical, and discarding them will not influence the equivalence of measuring other qubits. For q-equivalence, we should ensure that the tensors corresponding to every pair of qubits satisfy the requirement for q-equivalence, that is, the remaining tensor do not depend on the measurement indices, and the tensors of the two circuits are also identical. Then, such pairs of tensors can be discarded.

This qubit-by-qubit partition can help us reduce the number

of tensors needed to be considered at the same time. If there are still tensors that cannot be discarded, then they should be collected and contracted and checked using the basic algorithms. The effectiveness of this optimisation scheme has been confirmed in experiments (see Sec. V).

V. NUMERICAL RESULTS

In this section, we evaluate the effectiveness of our algorithms, with the aim to confirm that no significant time and space consumption will be incurred from embedding classical logic into conventional quantum circuits. More precisely, we compare our equivalence checking algorithms for dynamic quantum circuits with the TDD-based equivalence checking method for conventional quantum circuits. In addition, we also implemented the optimised algorithms based on qubit-by-qubit partition and compared them with the basic algorithms.

Benchmarks. We choose the dynamic quantum circuits of some commonly used algorithms such as quantum Fourier transform (QFT) [31], phase estimation (PE) [5] and circuits for error correction [32], teleportation [26] and state injection [4]. For each circuit, we compare them with the corresponding conventional quantum circuits given in [26]. We then check m-equivalence for the quantum Fourier transform and phase estimation circuits and check q-equivalence for the error correction, teleportation, and state injection circuits.

Implementation. In our experiments, for each pair of conventional quantum circuit C and its corresponding dynamic circuit C' , we calculate the TDD representations of C and C' and check their equivalence by comparing these two TDDs. To this end, we employ the TDD package provided in [23]. All the verification algorithms are implemented using Python3 and the experiments are conducted on a laptop with Intel i7-1065G7 CPU and 8GB RAM.

A. Comparison with EC of Conventional Quantum Circuits

Baseline. We compare the time and memory consumption of our verification algorithms with the TDD-based equivalence checking method proposed in [23] for conventional quantum circuits. Note that the latter cannot deal with dynamic quantum circuits. So we isolate from our algorithms the module for constructing TDD representations of dynamic circuits, and compare it with the module of the algorithm in [23] which constructs TDD representations of the corresponding conventional circuits. This comparison is fair, as both our algorithms and the algorithm in [23] need to construct two such TDDs and, once the TDDs are computed, the time/memory consumption of equivalence checking is negligible.

Results. Table I gives the experiment results, where columns ‘Basic Alg.’ and ‘Alg. in [23]’ record the time and memory consumption in generating TDD representations for a dynamic circuit by our basic algorithms and the corresponding conventional circuit by the compared algorithm, respectively. From the table we can see that our basic algorithms run as effectively as the equivalence checking algorithm for conventional quantum circuits, and the maximum number of the nodes of the TDDs constructed in the calculation process

TABLE I
EXPERIMENT RESULTS

	Benchmarks	Basic Alg.			Optimised Alg.			Alg. in [23]	
		tdd_time(s)	time(s)	m_nodes	time(s)	m_nodes	tdd_time(s)	nodes	
m- eq	qft_2	0.00	0.01	8	0.01	6	0.00	7	
	qft_3	0.01	0.03	15	0.01	10	0.01	15	
	qft_4	0.02	0.04	31	0.02	18	0.02	31	
	qft_5	0.05	0.08	63	0.03	34	0.03	63	
	qft_6	0.08	0.13	127	0.06	66	0.05	127	
	qft_7	0.16	0.27	255	0.10	130	0.09	255	
	qft_8	0.32	0.52	511	0.18	258	0.19	511	
	qft_9	0.51	0.87	1023	0.34	514	0.34	1023	
	qft_10	1.45	2.65	2047	0.72	1026	1.19	2047	
	qft_11	2.79	4.59	4095	1.34	2050	1.79	4095	
	qft_12	7.71	11.21	8191	2.96	4098	3.46	8191	
	qft_13	13.74	19.83	16383	5.81	8194	6.03	16383	
	qft_14	28.01	39.80	32767	10.59	16386	11.66	32767	
	qft_15	53.76	75.08	65535	20.87	32770	21.18	65535	
	qft_16	119.31	158.57	131071	42.54	65538	39.00	131071	
q- eq	PE_2	0.01	0.03	20	0.01	11	0.01	20	
	PE_3	0.03	0.07	58	0.03	23	0.03	58	
	PE_4	0.16	0.28	180	0.06	47	0.09	180	
	PE_5	0.31	0.84	614	0.11	95	0.4	614	
	PE_6	1.32	2.41	2248	0.19	191	0.56	2248	
	PE_7	1.01	3.34	2664	0.32	383	1.80	762	
	Bitflip	0.01	0.06	108	0.03	50	0.03	108	
	Phaseflip	0.01	0.10	108	0.06	51	0.06	108	
	Teleportation	0.00	0.03	20	0.02	14	0.01	20	
	State_inject_S	0.00	0.01	10	0.01	8	0.01	10	
	State_inject_T	0.01	0.02	10	0.01	8	0.01	10	

* The ‘nodes’ column records the numbers of nodes in the TDDs of the circuit and the ‘m_nodes’ columns record the maximum numbers of nodes of the TDDs constructed in the calculation process.

* The ‘tdd_time’ columns record the time for constructing the TDDs for the circuits, and the ‘time’ columns record the time for running the algorithm (including TDD construction time).

is very close to the number of nodes of the final TDD representation of the circuit.

B. Comparison of the Optimised and Basic Algorithms

We also implemented two optimised algorithms for m- and q-equivalence checking, that is, the qubit-by-qubit equivalence checking method proposed in Sec. IV-D, and then compare them with the basic algorithms.

Results. Results of the optimised methods are recorded in column ‘Optimised Alg.’ of Table I, where we can see that the optimised algorithms can significantly reduce the time/space consumption of the equivalence checking process. Consider the circuit qft_16 as an example. The basic algorithm takes 119 seconds with the maximal number of nodes appeared during the process being 131,071. In comparison, the optimised algorithm only takes 42.54 seconds with a maximum of 65,538 nodes. Thus, this optimisation method can really help in reducing the time and space consumption of the algorithms.

VI. CONCLUSION

Dynamic quantum circuits have been introduced as an effective method for executing quantum algorithms on near-term quantum devices. In this paper, we gave a formal definition of dynamic quantum circuits and proposed to characterise their functionalities in terms of ensembles of linear operators. Based on this novel semantics, two dynamic quantum circuits are equivalent if they have the same functionality. We further introduced two special kinds of equivalences for dynamic quantum circuits and implemented two equivalence checking algorithms based on the tensor decision diagram representations of dynamic quantum circuits. Experiments show that these algorithms are as efficient as the corresponding algorithms for conventional quantum circuits.

In the future, we will explore methods like employing an optimal contraction order to further improve the performance of our equivalence checking algorithms. Another open question is to devise effective algorithms for checking the equivalence of general dynamic quantum circuits, which requires calculating partial traces and thus advanced tensor network contraction techniques like that introduced in [33] may help.

REFERENCES

- [1] J. Preskill, “Quantum computing in the NISQ era and beyond,” *Quantum*, vol. 2, p. 79, 2018.
- [2] S. Wehner, D. Elkouss, and R. Hanson, “Quantum internet: A vision for the road ahead,” *Science*, vol. 362, no. 6412, 2018.
- [3] S. Endo, Z. Cai, S. C. Benjamin, and X. Yuan, “Hybrid quantum-classical algorithms and quantum error mitigation,” *Journal of the Physical Society of Japan*, vol. 90, no. 3, p. 032001, 2021.
- [4] C. A. Ryan, B. R. Johnson, D. Ristè, B. Donovan, and T. A. Ohki, “Hardware for dynamic quantum computing,” *Review of Scientific Instruments*, vol. 88, no. 10, p. 104703, 2017.
- [5] A. D. Corcoles, M. Takita, K. Inoue, S. Lekuch, Z. K. Minev, J. M. Chow, and J. M. Gambetta, “Exploiting dynamic quantum circuits in a quantum algorithm with superconducting qubits,” *arXiv:2102.01682*, 2021.
- [6] M. Barrett, J. Chiaverini, T. Schaetz, J. Britton, W. Itano, J. Jost, E. Knill, C. Langer, D. Leibfried, R. Ozeri *et al.*, “Deterministic quantum teleportation of atomic qubits,” *Nature*, vol. 429, no. 6993, pp. 737–739, 2004.
- [7] M. Riebe, H. Häffner, C. Roos, W. Hänsel, J. Benhelm, G. Lancaster, T. Körber, C. Becher, F. Schmidt-Kaler, D. James *et al.*, “Deterministic quantum teleportation with atoms,” *Nature*, vol. 429, no. 6993, pp. 734–737, 2004.
- [8] L. Steffen, Y. Salathe, M. Oppliger, P. Kurpier, M. Baur, C. Lang, C. Eichler, G. Puebla-Hellmann, A. Fedorov, and A. Wallraff, “Deterministic quantum teleportation with feed-forward in a solid state system,” *Nature*, vol. 500, no. 7462, pp. 319–322, 2013.
- [9] K. S. Chou, J. Z. Blumoff, C. S. Wang, P. C. Reinhold, C. J. Axline, Y. Y. Gao, L. Frunzio, M. Devoret, L. Jiang, and R. Schoelkopf, “Deterministic teleportation of a quantum gate between two logical qubits,” *Nature*, vol. 561, no. 7723, pp. 368–373, 2018.
- [10] P. Reinhold, S. Rosenblum, W.-L. Ma, L. Frunzio, L. Jiang, and R. J. Schoelkopf, “Error-corrected gates on an encoded qubit,” *Nature Physics*, vol. 16, no. 8, pp. 822–826, 2020.
- [11] Z. K. Minev, S. O. Mundhada, S. Shankar, P. Reinhold, R. Gutiérrez-Jáuregui, R. J. Schoelkopf, M. Mirrahimi, H. J. Carmichael, and M. H. Devoret, “To catch and reverse a quantum jump mid-flight,” *Nature*, vol. 570, no. 7760, pp. 200–204, 2019.
- [12] D. Gottesman, “An introduction to quantum error correction and fault-tolerant quantum computation,” in *Quantum information science and its contributions to mathematics, Proceedings of Symposia in Applied Mathematics*, vol. 68, 2010, pp. 13–58.
- [13] A. Paler, I. Polian, K. Nemoto, and S. J. Devitt, “Fault-tolerant, high-level quantum circuits: form, compilation and description,” *Quantum Science and Technology*, vol. 2, no. 2, p. 025003, 2017.
- [14] N. Ofek, A. Petrenko, R. Heeres, P. Reinhold, Z. Leghtas, B. Vlastakis, Y. Liu, L. Frunzio, S. Girvin, L. Jiang *et al.*, “Extending the lifetime of a quantum bit with error correction in superconducting circuits,” *Nature*, vol. 536, no. 7617, pp. 441–445, 2016.
- [15] D. Ristè, C. Bultink, K. W. Lehnert, and L. DiCarlo, “Feedback control of a solid-state qubit using high-fidelity projective measurement,” *Physical Review Letters*, vol. 109, no. 24, p. 240502, 2012.
- [16] S. Bravyi, D. Browne, P. Calpin, E. Campbell, D. Gosset, and M. Howard, “Simulation of quantum circuits by low-rank stabilizer decompositions,” *Quantum*, vol. 3, p. 181, 2019.
- [17] D. Riste, M. Dukalski, C. Watson, G. De Lange, M. Tiggelman, Y. M. Blanter, K. W. Lehnert, R. Schouten, and L. DiCarlo, “Deterministic entanglement of superconducting qubits by parity measurement and feedback,” *Nature*, vol. 502, no. 7471, pp. 350–354, 2013.
- [18] O.-P. Saira, J. Groen, J. Cramer, M. Meretska, G. De Lange, and L. DiCarlo, “Entanglement genesis by ancilla-based parity measurement in 2d circuit qed,” *Physical Review Letters*, vol. 112, no. 7, p. 070502, 2014.
- [19] C. K. Andersen, A. Remm, S. Lazar, S. Krinner, J. Heinsoo, J.-C. Besse, M. Gabureac, A. Wallraff, and C. Eichler, “Entanglement stabilization using ancilla-based parity detection and real-time feedback in superconducting circuits,” *npj Quantum Information*, vol. 5, no. 1, pp. 1–7, 2019.
- [20] P. Niemann, R. Wille, D. M. Miller, M. A. Thornton, and R. Drechsler, “Qmdds: Efficient quantum function representation and manipulation,” *IEEE Transactions on Computer-Aided Design of Integrated Circuits and Systems*, vol. 35, no. 1, pp. 86–99, 2015.
- [21] G. F. Viamontes, I. L. Markov, and J. P. Hayes, “Checking equivalence of quantum circuits and states,” in *2007 IEEE/ACM International Conference on Computer-Aided Design*. IEEE, 2007, pp. 69–74.
- [22] L. Burgholzer and R. Wille, “Improved dd-based equivalence checking of quantum circuits,” in *2020 25th Asia and South Pacific Design Automation Conference (ASP-DAC)*. IEEE, 2020, pp. 127–132.
- [23] X. Hong, X. Zhou, S. Li, Y. Feng, and M. Ying, “A tensor network based decision diagram for representation of quantum circuits,” *arXiv:2009.02618*, 2020.
- [24] X. Hong, M. Ying, Y. Feng, X. Zhou, and S. Li, “Approximate equivalence checking of noisy quantum circuits,” in *58th Design Automation Conference (DAC)*. ACM, 2021.
- [25] R. E. Bryant, “Symbolic boolean manipulation with ordered binary-decision diagrams,” *ACM Computing Surveys (CSUR)*, vol. 24, no. 3, pp. 293–318, 1992.
- [26] M. A. Nielsen and I. L. Chuang, *Quantum Computation and Quantum Information*. Cambridge University Press, 2000.
- [27] M. Ying, *Foundations of Quantum Programming*. Morgan Kaufmann, 2016.
- [28] I. L. Markov and Y. Shi, “Simulating quantum computation by contracting tensor networks,” *SIAM Journal on Computing*, vol. 38, no. 3, pp. 963–981, 2008.
- [29] J. Biamonte, “Lectures on quantum tensor networks,” *arXiv:1912.10049*, 2019.
- [30] E. Pednault, J. A. Gunnels, G. Nannicini, L. Horesh, T. Magerlein, E. Solomonik, and R. Wisnieff, “Breaking the 49-qubit barrier in the simulation of quantum circuits,” *arXiv:1710.05867*, vol. 15, 2017.
- [31] R. B. Griffiths and C.-S. Niu, “Semiclassical fourier transform for quantum computation,” *Physical Review Letters*, vol. 76, no. 17, p. 3228, 1996.
- [32] S. J. Devitt, W. J. Munro, and K. Nemoto, “Quantum error correction for beginners,” *Reports on Progress in Physics*, vol. 76, no. 7, p. 076001, 2013.
- [33] F. Pan, P. Zhou, S. Li, and P. Zhang, “Contracting arbitrary tensor networks: General approximate algorithm and applications in graphical models and quantum circuit simulations,” *Physical Review Letters*, vol. 125, p. 060503, Aug 2020.